

## Electrophoretic Characterization of Transient Photochemical Reaction Products

Mary Jane Gordon, Eric Okerberg,  
Michael L. Gostkowski, and Jason B. Shear\*

Department of Chemistry & Biochemistry  
The Institute for Cellular & Molecular Biology and  
The Center for Nano & Molecular Science & Technology  
The University of Texas, Austin, Texas 78712

Received August 20, 2001

Fluorescence can provide exquisite sensitivity for tracking fast solution-phase reactions, but often does not yield detailed information regarding unknown molecular structures. Although mass analysis has been valuable as a complement to spectroscopy for analyzing transient gas-phase products, mass spectrometry of aqueous reaction intermediates is limited by the speed at which components can be transferred from the reaction site to the gas phase—currently, tens of milliseconds at best.<sup>1</sup> In this communication, we demonstrate that unstable aqueous samples can be *electrophoretically* profiled within  $\sim 1$  ms of their production, providing the means to infer product charge states before these components decay. Our results suggest that multiphoton-excited (MPE) photochemistry of serotonin (5-hydroxytryptamine, *5HT*) and related molecules creates fluorescent radicals that degrade in tens of milliseconds.

When 5-hydroxyindoles are irradiated with tightly focused near-IR output from a femtosecond laser, visible fluorescence is produced in a process comprised of two principal steps: a four-photon excited photochemical reaction, and fluorescence excitation of photoproducts via absorption of two additional photons.<sup>2</sup> Because these products can be more readily detected than their weakly fluorescent parent indoles, MPE photochemistry has been used for zeptomole analysis after fractionation with capillary electrophoresis (CE).<sup>3</sup>

5-Hydroxyindole photoproducts form rapidly (probably within hundreds of nanoseconds) within multiphoton reaction regions ( $\sim 1 \mu\text{m}^3$ ). In addition, much is known about the conditions that favor photoproduct generation. For example, Good's buffers have been shown to augment photoderivatization, while the presence of molecular oxygen appears to deactivate a relatively long-lived ( $\tau > 10$  ns) intermediate state.<sup>3</sup> These spectroscopic studies, however, have not provided solid evidence to implicate a particular photoreaction mechanism. Importantly, the poor thermal stability of 5-hydroxyindole photoproducts has thwarted attempts to generate and collect sufficient quantities of material for subsequent mass-spectrometric or NMR analysis.<sup>3</sup>

To examine the charge state of transient photoproducts, we have adapted optically gated CE<sup>4</sup> to characterize femtoliter MPE reaction packets on millisecond time scales. Here, a large applied electric field rapidly transports products from a reaction site to a probe site only micrometers away (Figure 1A,B) at velocities that reveal molecular charge-to-drag ratios. The instrument designed for these studies is shown in Figure 1C. Modelocked output (780 nm) from a 80-MHz titanium:sapphire laser is split, with part of the beam directed through a Pockel's cell for optical switching. This beam is recombined slightly off-axis with the unmodulated

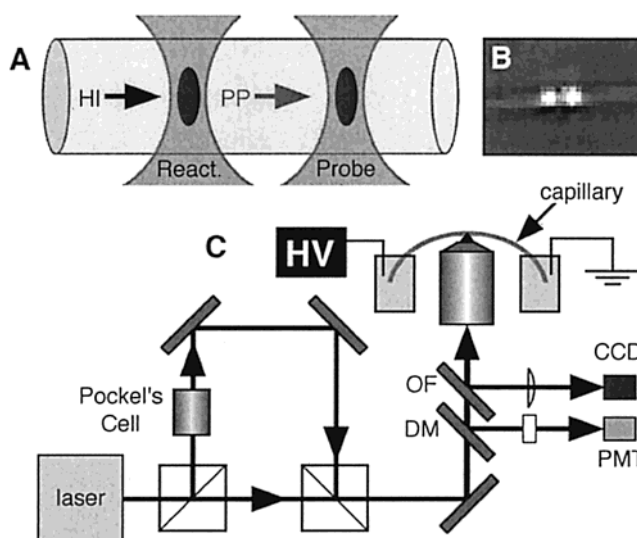


**Figure 1.** Charge-characterization strategy. (A) Hydroxyindoles (HI) enter the reaction focal volume, where they undergo rapid conversion to fluorescent photoproducts (PP). A product migrates to the probe site at a velocity  $v$ ,  $v = \mu_e E + v_{eo}$ , where  $\mu_e$  is the electrophoretic mobility,  $E$  is the electric field, and  $v_{eo}$  is the electroosmotic velocity. (B) Saturated image of laser focal spots within a  $4.7\text{-}\mu\text{m}$  i.d. channel, which appears as a horizontal band. (C) A laser beam is split, with one portion switched to high intensity for  $200\text{-}\mu\text{s}$  periods. The recombined (but slightly noncollinear) beams pass through a dichroic mirror (DM) and an optical flat (OF) before being focused by an objective into the capillary. Video (CCD) imaging helps align the focal spots; collected fluorescence is reflected by DM, passes through visible filters, and is measured with a PMT and a multichannel scaler.

beam, and both are directed through a dichroic mirror into an oil-immersion objective.

Because the modulated and unmodulated beams are not exactly collinear, the two beam waists are formed at different positions in the focal plane. A  $4.7\text{-}\mu\text{m}$  i.d. fused-silica capillary is secured to the top surface of a coverslip mounted on an adjustable stage, and the laser beam focal spots are positioned within the channel by using a video imaging system to guide alignment. Separation of the two focal spots can be varied with micrometer resolution to a maximum distance of  $\sim 15 \mu\text{m}$ . The modulated beam is switched to high power (several hundred milliwatts) for  $200\text{-}\mu\text{s}$  periods to generate photoreaction packets. The unmodulated probe beam is held at a level severalfold lower to minimize generation of photoproducts (and attendant background fluorescence) at the detection site. Sample solutions ( $500 \mu\text{M}$ ) in  $20$  mM HEPES buffer (pH 7.0) are continuously transported through the capillary by electroosmosis and electrophoresis.

Surprisingly, earlier studies found that positive (*5HT*), neutral (5-hydroxytryptophan, *5HTrp*), and negative (5-hydroxyindole-3-acetic acid, *5HIAA*) compounds (Figure 2A) each yield a positively charged fluorescent photoproduct that can be observed  $0.1$  to  $1$  s after the reactions are initiated.<sup>5</sup> In addition, *5HIAA* generates several slower migrating products.

Strikingly different results are obtained on the much faster time scale of the current studies, indicating that important chemical changes take place between  $\sim 1$  ms and  $0.1$  s after reaction initiation. Figure 2B shows a scaled overlay of separate analyses of *5HT*, *5HTrp*, and *5HIAA* photoproducts, where reaction products were transported electrophoretically over  $\sim 12(\pm 1) \mu\text{m}$ . These data reveal distinct maxima for each species and only one fluorescent product for each reaction (it is possible that better

(1) Paiva, A. A.; Tilton, R. F., Jr.; Crooks, G. P.; Huang, L. Q.; Anderson, K. S. *Biochemistry* **1997**, *36*, 15472–15476.

(2) Shear, J. B.; Xu, C.; Webb, W. W. *Photochem. Photobiol.* **1997**, *65*, 931–936.

(3) Gostkowski, M. L.; Currey, T. E.; Okerberg, E.; Kang, T. J.; Vanden Bout, D. A.; Shear, J. B. *Anal. Chem.* **2000**, *72*, 3821–3825. Gostkowski, M. L. Ph.D. Dissertation, University of Texas, Austin, TX, 2000.

(4) Monnig, C. A.; Jorgenson, J. W. *Anal. Chem.* **1991**, *63*, 802–807.

(5) Gordon, M. J.; Shear, J. B. *J. Am. Chem. Soc.* **2001**, *123*, 1790–1791.

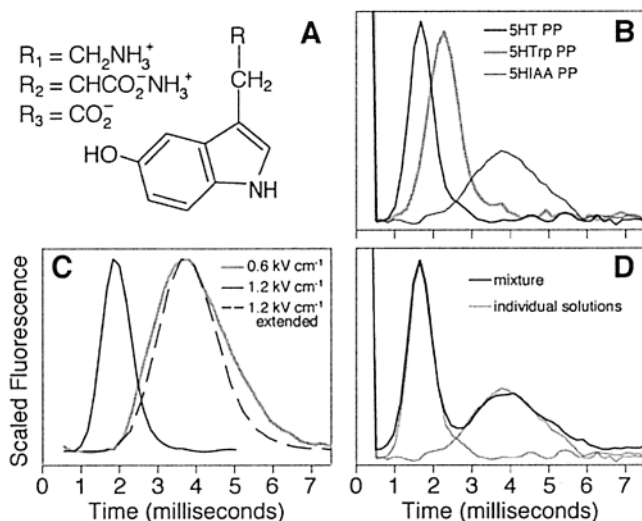


**Figure 2.** Electrophoretic analyses of hydroxyindole photoproducts. (A) Structures of *5HT* ( $R_1$ ), *5HTrp* ( $R_2$ ), and *5HIAA* ( $R_3$ ). (B) Analysis of photoproducts (PP) generated from *5HT*, *5HTrp*, and *5HIAA*. Photoproducts were created in individual solutions and electrophoretically transported to a detection site micrometers away. Data bin size is  $\sim 164 \mu\text{s}$ , and data were subjected to a three-point running smooth. (C) Electrophoretic analysis of *5HTrp* photoproduct with different fields. The dashed trace represents a 2-fold horizontal expansion of the high-field data to allow direct visual comparison of *spatial* bandwidths. (D) Electrophoretic fractionation of photoreaction products generated from a mixture of *5HT* and *5HIAA*, with the individual analyses of *5HT* and *5HIAA* from part B shown in gray. B, C, and D are an average of several thousand electrophoretic analyses; B and D were performed at  $1.1 \text{ kV cm}^{-1}$ .

electrophoretic resolution, sensitivity, or spectral discrimination would reveal additional components). The order in which photoproducts arrive at the detection site clearly correlates with the charge of the parent hydroxyindoles, a result not obtained at longer time scales.<sup>5</sup>

The magnitude of electroosmotic flow was established by measuring the time required for a nonfluorescent buffer plug to migrate from the capillary inlet to the focal spots in a capillary filled with buffered *5HTrp*. The flow rate was experimentally indistinguishable from the velocity of the *5HTrp* photoproduct (<4% difference), indicating that photoreaction does not alter the charge state of *5HTrp* in the first milliseconds after irradiation. Similarly, the electrophoretic mobilities ( $\mu_e$ ) calculated for *5HT* and *5HIAA* photoproducts,  $2.0$  and  $-2.0 \times 10^{-4} \text{ cm}^2 \text{ V}^{-1} \text{ s}^{-1}$ , respectively, are within experimental error ( $\sim 10\%$ ) of the mobilities measured for native *5HT* and *5HIAA*.

The principal contribution to spatial bandwidth in these studies is diffusion (Figure 2C). Bandwidth at half-maximum ( $\Delta x$ ) for the *5HTrp* photoproduct was examined by using  $0.6$  and  $1.2 \text{ kV cm}^{-1}$  ( $\sim 9 \mu\text{m}$  migration) and was found to scale nearly as the square root of the migration time ( $\Delta x_{0.6} / \Delta x_{1.2} \approx 1.3$ , vs  $1.4$  for a diffusion-limited process). With relatively minor modifications, this system should support fields  $> 50 \text{ kV cm}^{-1}$ , levels that have been useful for fractionating laser dyes over  $\sim 100 \mu\text{m}$  on millisecond time scales.<sup>6</sup> Adaptation of the current system to ultrahigh fields should extend electrophoretic analysis to the investigation of aqueous chemistry within microseconds of

reaction. With such improvements in speed, however, photogeneration times will need to be decreased to avoid increases in bandwidth.

Others have shown that 5-hydroxyindole dimers and trimers can be created via chemical and electrochemical oxidation.<sup>7</sup> If multimers were formed through photooxidation, their mobilities would be similar to the parent hydroxyindoles. To examine the possibility that the fluorescent products in the current studies are created through these condensation reactions, we have electrophoretically analyzed photochemical reactions containing a mixture of *5HT* and *5HIAA* (Figure 2D). In this case, multimer production would be evident by new components migrating at intermediate velocities (for a *5HT-5HIAA* heterodimer,  $\mu_e = 0$ ). Notably, no fluorescent bands are detected other than those seen in the individual analyses.

These results suggest a mechanism in which multiphoton excitation of a hydroxyindole molecule leads to the sequential loss of an electron and a proton, creating a fluorescent radical of the same charge and similar mass as the parent compound. Photophysical and photochemical studies offer additional support for this possible mechanism. First, we find that the optimal energy ( $E_{\text{max}}$ ) for two-photon fluorescence excitation of the *5HT* photoproduct,  $\sim 3.2 \text{ eV}$ ,<sup>3</sup> is similar to  $E_{\text{max}}$  for one-photon transient absorption by *5HTrp* radicals,  $\sim 3.0 \text{ eV}$ .<sup>8</sup> The small discrepancy between these energies is consistent with "blue-shifts" commonly reported for two-photon spectra of large chromophores in solution. Second, addition of the radical quencher, mercaptoethylamine,<sup>9</sup> to *5HT* solutions sharply decreases multiphoton-generated visible emission.<sup>3</sup> Third, alkyl substitution at the 3-position was not found to be critical to the photochemical process, a result that precludes the possibility that side-chain chemistry is inherent to these reactions. Interestingly, we find that saturation of hydroxyindole solutions with the efficient electron scavenger<sup>10</sup>  $\text{N}_2\text{O}$  decreases multiphoton-generated visible emission—possibly indicating that highly reactive species created by the quenching of solvated electrons (e.g., hydroxyl radicals) play a role in subsequent degradation of hydroxyindole photoproducts. Further photochemical studies are in progress to examine these reactions in greater detail.

We believe these are the first studies to probe the charge state of aqueous *reaction products* on low-millisecond time scales, a capability made possible by decreasing the dimensions of electrophoretic analysis toward its fundamental limits. It would be useful to bridge the time scale between the current studies and our earlier experiments<sup>5</sup> to investigate the decomposition of these early photoproducts and appearance of later species in detail. This goal cannot be achieved by simply reducing the electric field, as separation efficiencies would degrade to impracticable levels. Instead, modifications are being made to the instrumentation to enable the laser foci to be separated by distances of up to several hundred micrometers.

**Acknowledgment.** These studies were supported by the Kinship Foundation, the Robert A. Welch Foundation, the Alfred P. Sloan Foundation, the National Science Foundation, and the Eli Lilly Corp.

JA016898P

(7) Humphries, K. A.; Wrona, M. Z.; Dryhurst, G. *J. Electroanal. Chem.* **1993**, *346*, 377–403. Wrona, M. Z.; Dryhurst, G. *Chem. Res. Toxicol.* **1998**, *11*, 639–650.

(8) Javanovic, S. V.; Simic, M. G. *Life Chem. Rep.* **1985**, *3*, 124–130.

(9) Song, L.; Varma, C. A.; Verhoeven, J. W.; Tanke, H. J. *Biophys. J.* **1996**, *70*, 2959–2968.

(10) Jovanovic, S. V.; Steenken, S. J. *Phys. Chem.* **1992**, *96*, 6674–6679.

(6) Jacobson, S. C.; Culbertson, C. T.; Daler, J. E.; Ramsey, J. M. *Anal. Chem.* **1998**, *70*, 3476–3480.